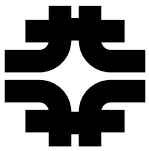

Fermi National Accelerator Laboratory

FERMILAB-Conf-95/201-E
CDF

Limits on Rare B Decays $\mathbf{B \to \mu^+\mu^-\, K^{\pm}}$ and $\mathbf{B \to \mu^+\mu^- K^{*0}}$

Carol Anway-Wiese
For the CDF Collaboration

Fermi National Accelerator Laboratory
P.O. Box 500, Batavia, Illinois 60510

Physics Department, University of California
Los Angeles, California 90024-1547

July 1995

Submitted to the Proceedings of the *XVII International Symposium on Lepton-Photon Interactions*, Beijing, China, August 10-15, 1995

Disclaimer

CDF/PUB/BOTTOM/PUBLIC/3248
Fermilab-Conf-95/201-E
July 15, 1995

Limits on Rare B Decays [1] $B \to \mu^+\mu^- K^\pm$ and $B \to \mu^+\mu^- K^{*0}$

Carol Anway-Wiese[2]
Representing the CDF Collaboration
Physics Department, University California, Los Angeles
405 Hilgard Ave, Los Angeles, California 90024-1547, USA

Abstract. We report on a search for flavor-changing neutral current decays of B mesons $B \to \mu^+\mu^- K^\pm$and $B \to \mu^+\mu^- K^{*0}$using data obtained in the Collider Detector at Fermilab (CDF) 1992-1993 data taking run. To reduce the amount of background in our data we use precise tracking information from the CDF silicon vertex detector to pinpoint the location of the decay vertex of the B candidate, and accept only events which have a large decay time. We compare this data to a B meson signal obtained in a similar fashion, but where the muon pairs originate from ψ decays, and calculate the relative branching ratios. In absence of any indication of flavor-changing neutral current decays we set an upper limits of BR($B \to \mu^+\mu^- K^\pm$) $< 1.1 \times 10^{-5}$, and BR($B \to \mu^+\mu^- K^{*0}$) $< 2.1 \times 10^{-5}$ at 90% confidence level, which are consistent with Standard Model expectations but leave little room for non-standard physics.

1 Introduction

Rare B decays provide us a way to test the Standard Model against possible effects of different form factors, anomalous magnetic moment of the $W^\pm$,

[1] Submitted to the Proceedings of the 17th International Symposium on Lepton Photon Interactions (LP95), Beijing, China, 1995.

[2] MS 318, Fermilab, PO Box 500 Batavia, IL 60510. caw@fnald.fnal.gov

and charged Higgs. Several theorists have predicted the rate of these decays. Differences in the form factors used in these calculations give relatively small uncertainties, but deviations from Standard Model physics can dramatically increase the expected rate. For a top quark mass of 150 GeV/c^2, A. Ali [1] predicts non-resonant branching ratios of BR($B \to \mu^+\mu^- K^\pm$) $= 4.4 \times 10^{-7}$ and BR($B \to \mu^+\mu^- K^{*0}$) $= 2.3 \times 10^{-6}$ using the hadronic matrix elements of Isgur and Wise [2]. G. Baillie [3] uses heavy quark effective theory to calculate the ratio of the decay rate in a portion of the non-resonant dimuon mass spectrum to the decay rate of $B \to \psi K, \psi \to \mu\mu$. The ratio is less sensitive to the uncertainties in the HQET calculation. The portion of the non-resonant dimuon mass spectrum he uses goes from $\hat{s} \equiv M(\mu\mu)^2/M_B^2 = 0.35$ to 0.48 and 0.50 to $\hat{s}_{max} = (M_B - M_K)^2/M_B^2$. He finds the ratio of the decay rates to be 2×10^{-3} for each decay mode at a top quark mass of 170 GeV/c^2. Burdman [4] has calculated the differential rates as a function of dimuon mass in the dimuon mass region 4.2 to 4.6 GeV/c^2 for $B \to \mu^+\mu^- K^\pm$, and 3.8 to 4.6 GeV/c^2 for $B \to \mu^+\mu^- K^{*0}$ since that is where form factor calculations are most accurate. He compares the Standard Model with several extensions. We present limits in these regions to constrain his calculations. We use the non-resonant theoretical differential decay rate as a function of dimuon mass from Isgur and Wise as calculated in [3] to extrapolate our results from the partial dimuon mass region to the overall non-resonant region.

2 Data and Method

At CDF [5] we have accurate momentum resolution in the central tracking chamber (CTC), further improved by using vertex position information from the silicon vertex detector (SVX) [6]. In this analysis we accept only pairs of muons which have traversed the SVX, the CTC, and have muon stubs in the central muon chambers (up to $\eta = 0.6$). Both muons must have $p_t(\mu) > 2.0$ GeV/c, and one $p_t(\mu) > 2.5$ GeV/c.

We select muon pairs with an invariant mass between 0.0 and 4.6 GeV/c^2, assign the K$^\pm$ and $\pi^\pm$ masses to tracks in the central tracking chamber and use a secondary vertex fit to help reconstruct candidate B's. Tight cuts on the vertex fit quality and the transverse proper decay time of the B candidate (0.1 mm) help reduce combinatoric background. Background from hadronic punch-through is largely reduced by requiring the B candidate to carry the majority of the momentum in a cone of 1.0 in ΔR, $\Delta R = \sqrt{\Delta\eta^2 + \Delta\phi^2}$. The transverse momentum cuts on the events are as follows: p_t(B) > 6.0 GeV/c, p_t(K^{*0}) > 2.0 GeV/c, and for $B \to \mu^+\mu^- K^\pm$, p_t(K) > 2.0 GeV/c. We assign

dimuons to the ψ resonance if their invariant mass falls between 3.016 and 3.132 GeV/c^2, and to the *(partial)* non-resonant region if their mass falls in the range 0.0 to 2.9, 3.3 to 3.6 or 3.8 to 4.6 GeV/c^2.

We constrain the three or four tracks of the B candidate to a common secondary vertex and constrain the direction of the secondary vertex away from the primary vertex to match the direction of the B candidate momentum (a pointing constraint). The B candidate mass spectra, shown in figures 1 and 5, show the $B \to \psi K^{\pm,*0}$ signal peaks and provide the slope and area of the sidebands for the background estimates. Seeing no evidence of signal in figures 2 and 6, we constrain the three or four tracks to the B meson mass and plot the dimuon mass spectra. Figures 3 and 4 show the dimuon mass spectra from $B \to \mu^+\mu^- K^\pm$ peak and sideband events, respectively, and figures 7 and 8 show the dimuon mass spectra from $B \to \mu^+\mu^- K^{*0}$ events. The signal events lie in the non-resonant regions in figures 3 and 7. The background estimate comes from the number of events in the non-resonant regions in figures 4 and 8, normalized to account for the large size of the B sidebands relative to the peak region. We obtain the number of ψ resonant events above background from the same figures.

3 $B \to \mu^+\mu^- K^\pm$ Results

After making the cuts we see 3 $B \to \mu^+\mu^- K^\pm$ candidate events in our non-resonant signal region (figure 3) which is consistant with the background estimate of 4.9 ± 1.4 events from figure 4. From these same figures, we see 34.2 ± 6.3 $B \to \psi K^\pm$ events above background. We correct the ratio of the number of non-resonant events to the number of resonant events with the relative efficiency and calculate the limit using the method of reference [8]. The designation *partial* indicates the dimuon mass regions 0.0 to 2.9, 3.3 to 3.6 and 3.8 to 4.6 GeV/c^2.

$$\frac{\mathrm{BR}(B \to \mu^+\mu^- K^\pm, partial)}{\mathrm{BR}(B \to \psi K^\pm, \psi \to \mu\mu)} < 0.13 \ \text{ at } \ 90\% \ \mathrm{CL}.$$

We extrapolate to the overall dimuon mass region by multiplying the partial branching ratios by 1.233 ± 0.001, as calculated using the RareB Monte Carlo and the theoretical models of Isgur and Wise[2, 3].

$$\frac{\mathrm{BR}(B \to \mu^+\mu^- K^\pm)}{\mathrm{BR}(B \to \psi K, \psi \to \mu\mu)} < 0.16 \ \text{ at } \ 90\% \ \mathrm{CL}.$$

Using $\mathrm{BR}(B \to \psi K^{\pm}, \psi \to \mu\mu) = 6.5 \pm 1.0 \times 10^{-5}$ [7], we can calculate the overall branching ratio limits.

$$\mathrm{BR}(B \to \mu^+\mu^- K^{\pm}, partial) < 0.9 \times 10^{-5} \text{ at } 90\% \text{ CL}$$

$$\mathrm{BR}(B \to \mu^+\mu^- K^{\pm}) < 1.1 \times 10^{-5} \text{ at } 90\% \text{ CL}.$$

For the special case Burdman [4] and others find useful, the limit from the dimuon mass region 4.2 to 4.6 GeV/c^2 is

$$\mathrm{BR}(B \to \mu^+\mu^- K^{\pm},\ 4.2 < m(\mu\mu) < 4.6\ \mathrm{GeV/c^2}) < 0.5 \times 10^{-5} \text{ at } 90\% \text{ CL}.$$

4 $B \to \mu\mu K^{*0}$ Results

After making the cuts we see 7 $B \to \mu^+\mu^- K^{*0}$ candidate events in our non-resonant signal region (figure 7) which is consistant with the background estimate of 9.2 ± 1.7 events from figure 8. In addition, we see 29.7 ± 6.0 $B \to \psi K^{*0}$ events above background.

$$\frac{\mathrm{BR}(B \to \mu^+\mu^- K^{*0}, partial)}{\mathrm{BR}(B \to \psi K^{*0}, \psi \to \mu\mu)} < 0.18 \text{ at } 90\% \text{ CL}.$$

We extrapolate to the overall dimuon mass region by multiplying the partial branching ratios by 1.289 ± 0.002, as above.

$$\frac{\mathrm{BR}(B \to \mu^+\mu^- K^{*0})}{\mathrm{BR}(B \to \psi K^{*0}, \psi \to \mu\mu)} < 0.23 \text{ at } 90\% \text{ CL}.$$

Using $\mathrm{BR}(B \to \psi K^{*0}, \psi \to \mu\mu) = 7.8 \pm 2.4 \times 10^{-5}$ [9], we can calculate the overall branching ratio limits.

$$\mathrm{BR}(B \to \mu^+\mu^- K^{*0}, partial) < 1.6 \times 10^{-5} \text{ at } 90\% \text{ CL}$$

$$\mathrm{BR}(B \to \mu^+\mu^- K^{*0}) < 2.1 \times 10^{-5} \text{ at } 90\% \text{ CL}.$$

In the upper end of the dimuon mass spectrum alone,

$$\mathrm{BR}(B \to \mu^+\mu^- K^{*0},\ 3.8 < m(\mu\mu) < 4.6\ \mathrm{GeV/c^2}) < 0.7 \times 10^{-5} \text{ at } 90\% \text{ CL}.$$

5 Acknowledgements

We thank Grant Baillie, UCLA, for his help in the theory behind the RareB Monte Carlo event generator and for many valuable discussions on the subject of rare B decays.

We thank the Fermilab staff and the technical staffs of the participating institutions for their vital contributions. This work was supported by the U.S. Department of Energy and National Science Foundation; the Italian Istituto Nazionale di Fisica Nucleare; the Ministry of Education, Science and Culture of Japan; the Natural Sciences and Engineering Research Council of Canada; the National Science Council of the Republic of China; the A. P. Sloan Foundation; and the Alexander von Humboldt-Stiftung.

References

[1] A. Ali, Phys. Lett. B 264 (1991) 447, Erratum, B 274 (1992) 526.

[2] N. Isgur and M. B. Wise, Phys. Lett. B 232 (1989) 113; and Phys. Lett. B 237 (1990) 527.

[3] G. Baillie, UCLA/93/TEP/26, hep-ph 9307369 (1993).

[4] G. Burdman, FERMILAB-Pub-95/113-T (1995).

[5] F. Abe *et al.* NIM A 271 (1988) 387, and references therein.

[6] B. Barnett *et al.* NIM A 315 (1992) 125.

[7] T. Browder, K. Honscheid, S. Playfer, CLNS 93/1261 (1994).

[8] O. Helene, NIM 212 (1983) 319; and G. Zech, NIM A 277 (1989) 608.

[9] Review of Particle Properties, Phys. Rev. D 45 (1992).

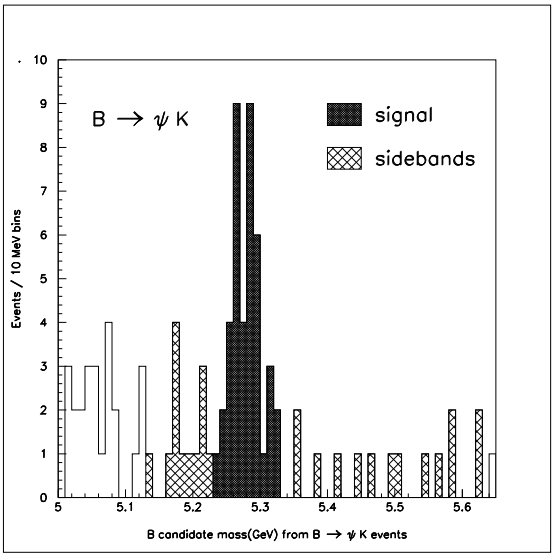

Figure 1: B candidate spectrum from $B \to \psi K^{\pm}$ decays. All cuts but the last fit probability cut constraining peak and sidebands to the center mass of same-sized bins.

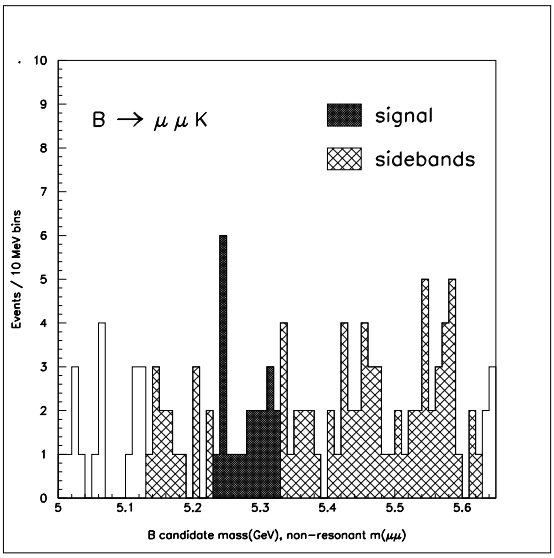

Figure 2: B candidate spectrum from $B \to \mu^+\mu^- K^{\pm}$ decays. All cuts but the last fit probability cut constraining peak and sidebands to the center mass of same-sized bins.

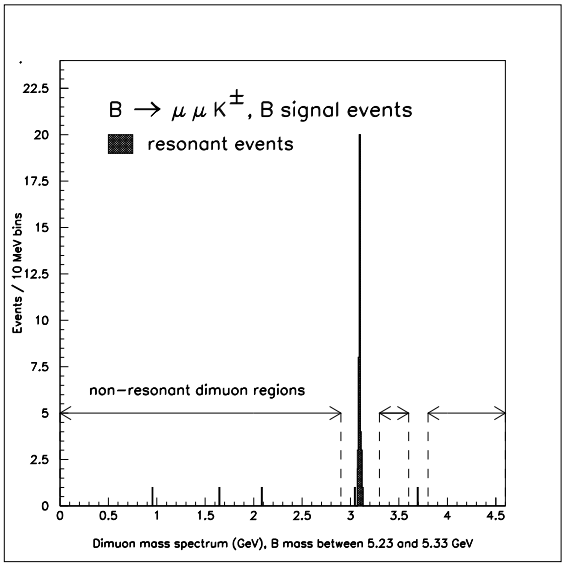

Figure 3: Dimuon mass spectrum from B peak events.

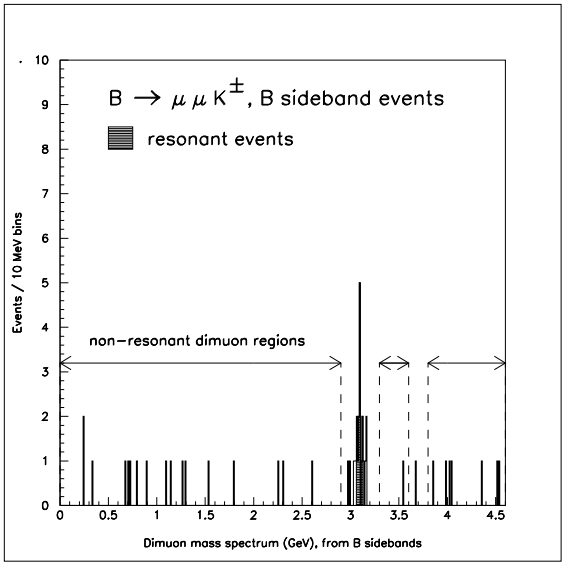

Figure 4: Dimuon mass spectrum from B sideband events.

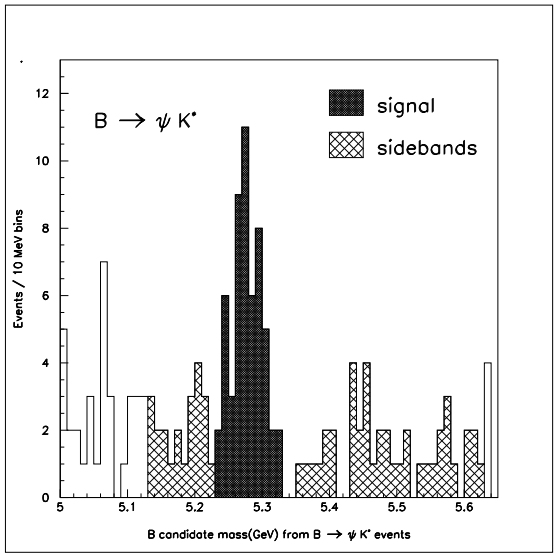

Figure 5: B candidate spectrum from $B \to \psi K^*$ decays. All cuts but the last fit probability cut constraining peak and sidebands to the center mass of same-sized bins.

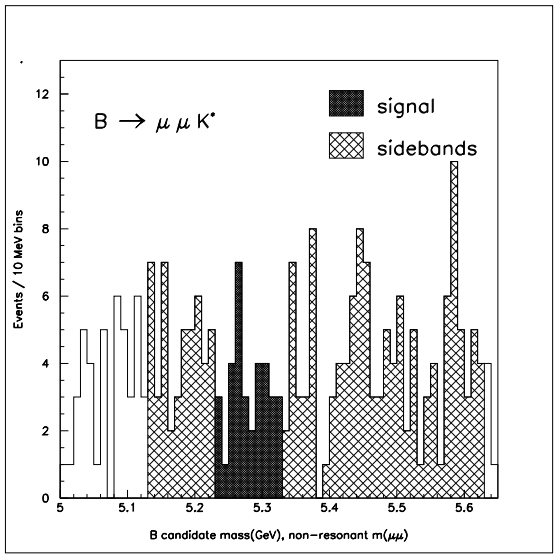

Figure 6: B candidate spectrum from $B \to \mu^+\mu^- K^{*0}$ decays. All cuts but the last fit probability cut constraining peak and sidebands to the center mass of same-sized bins.

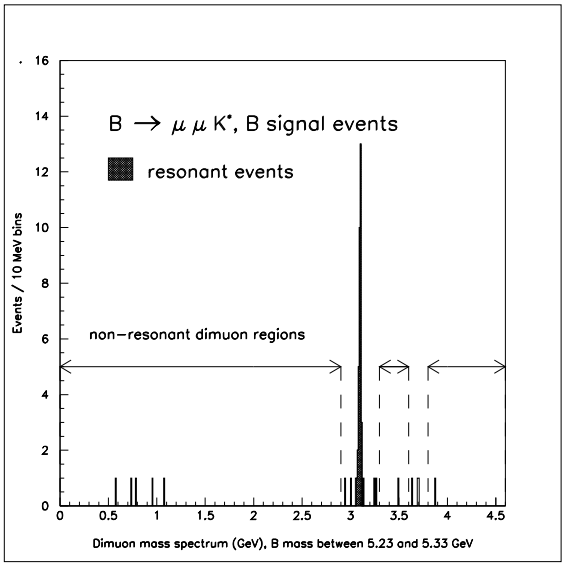

Figure 7: Dimuon mass spectrum from B peak events.

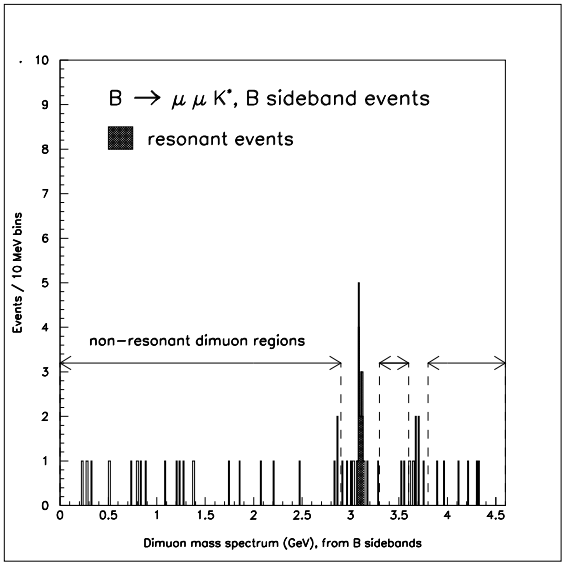

Figure 8: Dimuon mass spectrum from B sideband events.